Estuaries and Coasts
https://doi.org/10.1007/s12237-020-00790-5

SPECIAL ISSUE: HURRICANE SANDY IMPACTS AND RESPONSES

Tidal and Hurricane Impacts on Saltmarshes in the Northeastern Coastal and Barrier Network: Theory and Empirical Results

James T. Morris[1] · James Lynch[2] · Katherine A. Renken[1] · Sara Stevens[2] · Megan Tyrrell[3] · Holly Plaisted[2]

Received: 9 May 2019 / Revised: 28 May 2020 / Accepted: 19 June 2020

Abstract

The responses of marsh elevation in four National Parks affected by Hurricane Sandy were examined using empirical data from surface elevation tables (SET) and modeling. The parks examined were Fire Island National Seashore and Gateway National Recreational Area in New York; Cape Cod National Seashore, Massachusetts; and Assateague Island National Seashore, Maryland. Observed vertical accretion rates were compared with calculations made with the Marsh Equilibrium Model (MEM). MEM predicts vertical accretion resulting from the accumulation of organic material in soil and the capture of suspended inorganic material at the marsh surface. MEM simulations of a decade or more of marsh elevation change at 52 SET stations were generally consistent with observations. Park-specific averages of observed vertical accretion ranged from 0.16 ± 0.33 (± 1 SD) to 0.51 ± 0.21 cm/year, while the range of calculated rates was 0.15 ± 0.03 to 0.22 ± 0.05 cm/year, depending on the park. Grand means of observed and calculated rates were 0.36 ± 0.34 and 0.19 ± 0.06 cm/year, respectively. We defined a novel metric termed normalized elevation capital (NEC) that incorporates information about tide range and elevation capital. All but 2.3% of biomass collections from all the parks fell within 0 < NEC < 1. Consistent with marsh equilibrium theory, long-term vertical accretion rate tended to be greatest, 0.4 ± 0.2 cm/year, in the range 0.4 < NEC < 0.6 where vertical accretion is dominated by organic production. Average episodic accretion during the storm from mineral deposition also was greatest and positive, 0.6 ± 0.9 cm in the range 0.4 < NEC < 0.6. Finally, one marsh in Gateway NRA, restored by an application of sediment to NEC = 0.55–0.68, had post-treatment vertical accretion rates of 0.36 ± 0.31 cm/year, not statistically different from SET stations elsewhere in Gateway, 0.57 ± 0.54 cm/year. The sediment amendment placed restored sites in the range of NEC where theory predicts that biogenic accretion should dominate vertical accretion. Model simulations suggest that current rates of vertical accretion in the parks are close to their theoretical limits, and in the absence of new sediment, extant marsh communities in these parks are unlikely to survive continued acceleration of sea-level rise in the absence of periodic sediment renourishment.

Keywords Hurricane Sandy · Marsh vertical accretion · Marsh equilibrium theory · Resilience · MEM · Thin-layer placement · Restoration

Communicated by Dennis F. Whigham

Electronic supplementary material The online version of this article (https://doi.org/10.1007/s12237-020-00790-5) contains supplementary material, which is available to authorized users.

✉ James T. Morris
morris@biol.sc.edu

[1] Baruch Institute, University of South Carolina, Columbia, SC 29208, USA

[2] NPS, Northeast Coastal and Barrier Network, Kingston, RI 02881, USA

[3] North Atlantic Conservation Cooperative, US Fish and Wildlife Service, Hadley, MA 01035, USA

Introduction

On October 29, 2012, Hurricane Sandy made landfall near Atlantic City, NJ. Assateague Island and Cape Cod, MA, national seashores were inundated between 0.6 and 1.2 m locally, while Fire Island National Seashore and the Jamaica Bay unit of Gateway National Recreation Area, NY, experienced between 1.2 and 1.8 m of inundation due to storm surge (Blake et al. 2013). The greatest inundation, approximately 2.7 m, was recorded in New Jersey. Hurricane Sandy was the deadliest tropical storm outside of the southern United States since Hurricane Agnes in 1972, with 41 deaths directly caused by the storm surge and 72 total deaths directly attributed to all storm-related causes (Blake et al. 2013).

Published online: 23 July 2020

Additionally, an estimated 650,000 homes were damaged or destroyed and total damage estimates were in the tens of billions of dollars, an overwhelming portion of which was related to Hurricane Sandy's storm surge (Blake et al. 2013).

In the affected areas, there are saltmarshes in four national parks. Here we report results of a study of the response of these saltmarshes to Hurricane Sandy and assess their status with respect to differences in tidal dynamics and rising sea level. Tidal marshes provide valuable ecosystem services to humans including prevention of damage from storm surge and decreased damage to infrastructure (Costanza et al. 2006; Arkema et al. 2013). The four parks in our study—Assateague Island National Seashore (ASIS), Cape Cod National Seashore (CACO), Fire Island National Seashore (FIIS), and Gateway National Recreation Area (GATE)—together sheltered approximately 131,114 total acres of coastal habitat, and protected coastal populations and infrastructure on the coasts of Maryland, New York, and Massachusetts. A study by Narayan et al. (2017) estimated that the wetlands avoided $625 million in direct flood damages that would have resulted from Hurricane Sandy. However, storm impacts to the marshes and rising sea level may increase their vulnerability, which in turn will compromise their ability to protect coastal populations and infrastructure in the future.

We report here analyses of data collected by the parks from an array of Sediment Erosion Tables (SET). These observations were compared with predictions made with the Marsh Equilibrium Model (MEM) about current trends in the marshes, the risk from rising sea level, and generalities about the influence of key variables such as tide range and relative marsh elevation. We also compared observed accretion rates in marshes in the four parks before and after Hurricane Sandy, as well as the pre- and post-Sandy responses of a restoration site in GATE that had 0.4 to 0.5 m of sediment added followed by replanting in late 2003.

The Marsh Equilibrium Model

The one dimensional or point version of the Marsh Equilibrium Model (MEM) computes vertical accretion as a mass balance of mineral sediment and root inputs. It incorporates feedbacks among vegetation, sediments, and tides that enable a marsh to track sea level, within limits (Morris et al. 2002). Feedback between primary production and vertical accretion can be positive or negative, depending on the relative elevation of the marsh surface, and this is a function of the rate of sea-level rise. Relative marsh elevation and productivity determine the rate of vertical accretion (Fig. 1). The original model (Morris et al. 2002) has been modified so as to incorporate more variables that explicitly define processes that contribute to soil volume, such as below-ground biomass accumulation and the self-packing densities of organic and inorganic material in the soil (Morris et al. 2016). The accretion rate (cm/year) at a given point is a function of both organic and mineral inputs that alter the elevation (Z) of the surface such that

$$\frac{dz}{dt} = \frac{dz_{org}}{dt} + \frac{dz_{min}}{dt}$$

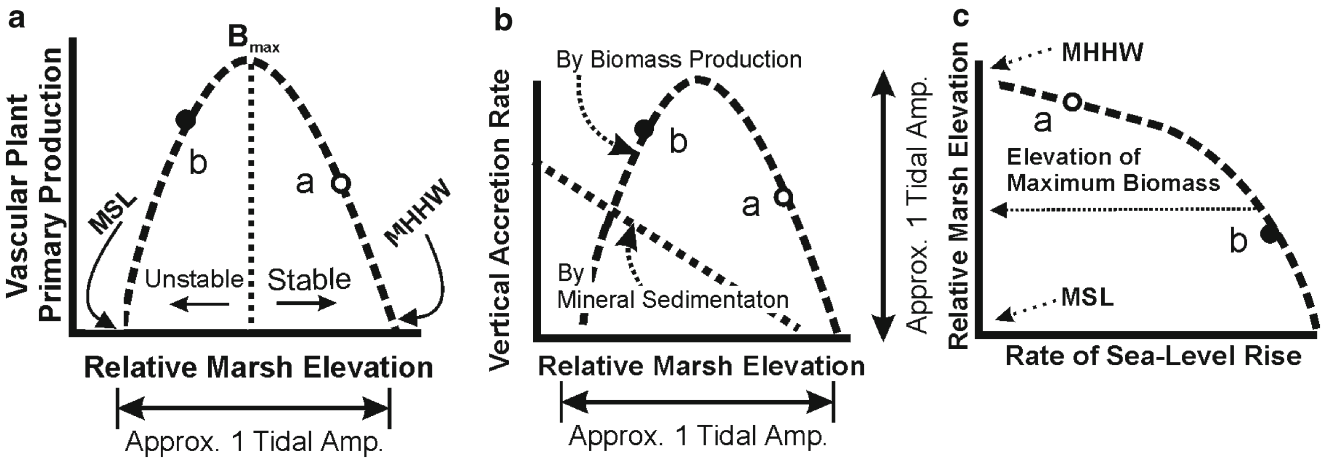

Fig. 1 Conceptual behavior of the Marsh Equilibrium Model. Shown in (A) is the relationship between primary production and relative marsh elevation. The feasible growth range spans a vertical dimension approximately between mean sea level (MSL) and mean higher high water (MHHW). Growth declines to zero at the extremes due to stress from hypoxia at the low end and osmotic stress at the high end. Elevations greater than the optimum (the elevation of B_{max}) are stable, e.g., the point a. Suboptimal elevations, e.g., point b, are unstable in the sense that when sea level rises (when relative elevation decreases), accretion by biomass production decreases as shown in (B) by the trajectory of point b. On the super-optimal side (point a), when sea level rises, both production and vertical accretion increase. In (B), the contributions of mineral sediment and biomass production to vertical accretion are shown. Biomass production is more important at higher elevations (see also Fig. 8). The equilibrium elevation will depend on the rate of sea-level rise as shown in (C). At super-optimal elevations, the equilibrium decreases slowly with rate of SLR because rising biomass compensates by raising the accretion rate. At suboptimal elevations (e.g., point b), the decrease in relative elevation is more rapid as a rising rate of sea level depresses productivity

The mineral contribution to soil volume is expressed as $\frac{dz_{min}}{dt} = \frac{0.5 \times q \times m \times f \times D \times F_{IT}}{k_2}$ where q is a unitless capture coefficient; m is the suspended sediment concentration expressed in g/cm^3; f is the flooding frequency or number of tides in a year, which is equal to 704 in a semi-diurnal location; D is the depth (cm) below mean high water (MHW), expressed as $D = \text{MHW} - Z$. The factor 0.5 takes into account that the average depth per tide is approximately ½ × D; F_{IT} is the fractional inundation time calculated as F_{IT} = (MHW−Z)/(MHW−MLW); $0 \le F_{IT} \le 1$. k_2 is the self-packing density of mineral sediment (= 1.99 g/cm^3, Morris et al. 2016). A limitation is that erosion is not treated explicitly by the model. Consequently, MEM cannot compute negative accretion rates. A more sophisticated model exists that couples MEM with the hydrodynamic model ADCIRC, with a major advantage being the dynamic computation of tidal datums across the estuarine landscape (Alizad et al. 2018).

The organic contribution to soil volume is expressed as $\frac{dz_{org}}{dt} = \frac{k_r \times R_{RS} \times B_{TR} \times Bs}{k_1}$

B_s is the peak above-ground biomass density (g/cm^2) in a given year, and coefficient k_r is the stable fraction of below-ground biomass. A typical value for *Spartina alterniflora* is $k_r = 0.1$, based on the lignin fraction of biomass (Hodson et al. 1984; Wilson et al. 1986; Buth and Voesenek 1987). R_{RS} is the root-to-shoot ratio (the ratio of total below-ground to above-ground biomass), $R_{RS} \cong 2$ (Darby and Turner 2008; Morris 1982); and B_{TR} is the turnover rate of below-ground biomass (year^{-1}), $B_{TR} \cong 0.5$. Rhizomes make up roughly half of the below-ground biomass (Morris 1982). They are perennial and have a much slower turnover rate than roots, so a turnover of 0.5/year for total below-ground biomass allows for a root turnover of about 1/year. Therefore, the above equation reduces to:

$\frac{dz_{org}}{dt} = \frac{0.1 \times B_s}{k_1}$, where k_1 is the self-packing density of organic material (0.085 g/cm^3). Above-ground biomass production does not contribute to vertical accretion as dead above-ground biomass and tends to be rafted out of the salt marsh on tides, exported as particulate and dissolved organic matter, or decomposed on the surface (Teal 1962; Chalmers et al. 1985; Bouchard and Lefeuvre 2000).

Study Areas

Our study focused on four National Parks managed within the Northeast Coastal and Barrier Network (NCBN) that contain saltmarshes—Assateague Island National Seashore (ASIS) in Maryland and Virginia, Cape Cod National Seashore (CACO) in Massachusetts, Fire Island National Seashore (FIIS) in New York, and Gateway National Recreation Area (GATE) in New York (Fig. 2).

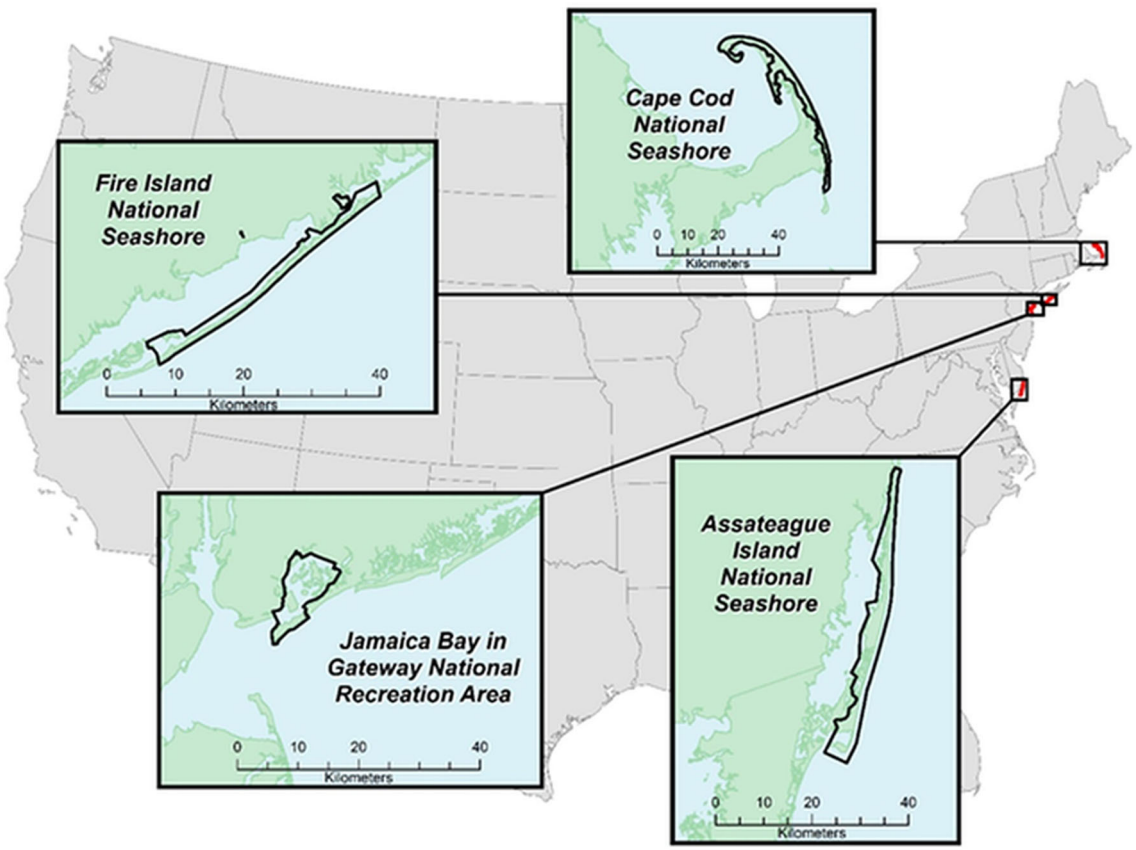

Fig. 2 Location of study sites

While the principles that control the evolution of the saltmarshes in the different parks are the same, there are substantial differences among parks in characteristics that control saltmarsh evolution, namely relative elevation, vegetation biomass, and tide range. The Gateway modeling efforts were focused on the Jamaica Bay unit and any reference to GATE refers to this unit and not the others located at Sandy Hook or Staten Island. There are three Sediment Elevation Table (SET) stations in GATE in a marsh that was restored in 2003 by thin-layer placement. Allowing 2 years for compaction of added sediment, the trend analyses reported here excluded SET data prior to 2005. Furthermore, one of the CACO sites is dominated by *Phragmites australis* in a tidally restricted area. This and other tidally restricted areas were excluded from the analyses reported here. Data from each park were synthesized in order to produce park- or site-specific values needed for the model.

Tide range varies among parks from less than 20 to 290 cm. Where available, tidal datums were determined using data from a Hobo pressure transducer, compensated for atmospheric pressure, and operated by James Lynch. Datums for sites on the west side of CACO were derived from recent tide data recorded at the NOAA gage in Boston, MA, station 8443970.

Sediment concentrations were available for all parks, but the number of observations, locations, timing, and methods of collection differed between parks. In some cases, only a few grab samples were collected at one time from creeks inside the park. FIIS was the only park reporting both inorganic and organic suspended sediment concentrations. Total suspended sediment data were reported elsewhere. In the case of GATE, the data were obtained from the Water Quality Visualization and Access Tool hosted by the Center for International Earth Science Information Network (CIESIN) of Columbia University (http://www.ciesin.columbia.edu/jbwq). Methodological details are available from the individual parks (CIESIN metadata) except for Gate. We summarized all of the available sediment data and for the simulations reported here, we use a constant, global average total inorganic sediment concentration of 15 mg/L.

Sea-Level Rise

The current rate of sea-level rise (SLR) assumed for all parks was derived from the monthly water level records of the three regional gages with the longest records (Battery, NY; Boston, MA; Atlantic City, NY). The Boston and Atlantic City monthly data were normalized to the annual mean 1950 level recorded at the Battery, NY, gage, aggregated, and a polynomial model (National Research Council 1987) was fitted to the combined data: $Y(t) = at + bt^2 + c$ where $Y(t)$ is the mean sea level (m), t is the cumulative month since January 1858, and the parameters a, b, and c are from a non-linear, least-squares fit to the combined data. The current rate of SLR was calculated from the first derivative of this equation at the current date ($t = 1934$ months): $\mathrm{SLR} = (a + 2bt)$ m/month. This returned a current rate of SLR of 0.39 cm/year (Fig. 3). The standard error ($\pm 4.75 \times 10^{-9}$) about the constant b gives a range of SLR of 0.37 to 0.42 cm/year.

Biomass

Peak biomass B_s is dependent on the elevation of the marsh and is calculated as a function of the depth (D) of the marsh surface below the mean high water (MHW) level:

$$B_s = aD + bD^2 + c$$

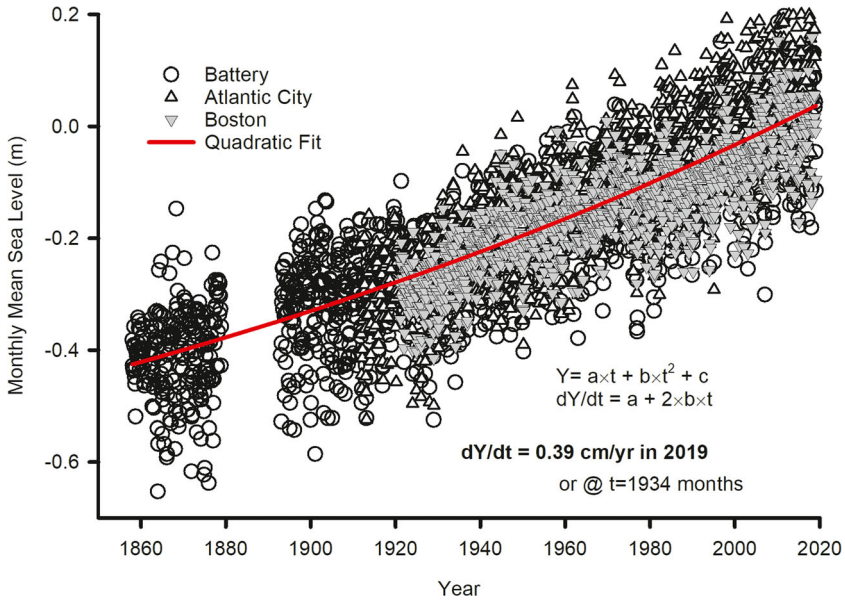

Fig. 3 Mean monthly sea level (m NAVD88) from NOAA's Battery, NY, station 8518750, Boston, MA, station 8443970, and Atlantic City, NJ, station 8534720 with a best fit of the quadratic $Y = \mathrm{at} + bt^2 + c$ where t is the cumulative number of months since January 1858, $a = 0.000166 \pm 0.00001$, $b = 4.19 \times 10^{-8} \pm 4.75 \times 10^{-9}$, $c = -.43066 \pm .0056$ (± 1 SE, $r^2 = 0.7$, $P < 0.0001$). The MSL data from Boston and Atlantic City were normalized to the 1950 annual mean sea level at Battery by subtracting 0.0099 m from the monthly Boston data and adding 0.3315 m to the monthly Atlantic City data

The coefficients, *a*, *b*, and *c* determine the shape of a parabolic growth curve describing the relationship between relative marsh elevation (expressed as depth below MHW) and the biomass density of *S. alterniflora*.

To determine parameters *a*, *b*, and *c* above-ground biomass, data were collected in conjunction with location and elevation data (by RTK) throughout the growth range of *S. alterniflora* in multiple locations in each park. In each park, the biomass data were grouped by elevation in 5 cm bins for fitting polynomial curves (Table S1). Methods for collecting biomass samples differed among parks, which was a limitation. Above-ground biomass samples and elevation data for ASIS were collected at 57 locations in the park in the fall of 2016 and at FIIS at a range of elevations in multiple marsh units. Above-ground biomass samples and elevation data at GATE were collected in 2012 by NPS staff, primarily in three marsh units. Above-ground and below-ground biomass samples and elevation data were collected by NPS staff in the eight marsh units at CACO in 2013 using a 3-in. diameter pipe.

A biomass growth curve was fitted for each park to the maximum biomass in each bin using PROC MODEL (SAS v 9.4). From the growth curves, the vertical range between the lower and upper growth limits varied from about 0.4 to 2 m (Fig. S1). Polynomial regressions generally described the distribution of maximum biomass in each park with R^2 values of 0.3 to 0.81. Data such as these confirm the importance of relative elevation and tide range as factors that constrain primary production, but they also remind us that other factors such as nutrients, hydrology, and sulfides are also important (Mendelssohn and Morris 2000). However, due to problems with the data, such as the non-uniform methodologies in which biomass samples were collected, we used the data primarily to generate a generic biomass growth curve, which was used in the model simulations as described below.

Normalized Elevation Capital

Parks in this study have marshes dominated by the saltmarsh cordgrass, *S. alterniflora*, which grows within a vertical range limited by hypoxia at the lower limit, and osmotic stress and soil salinity at the upper end (Mendelssohn and Morris 2000). The vertical range of *S. alterniflora* spans approximately between mean sea level (MSL) and mean high water (MHW) (McKee and Patrick Jr. 1988), and bioassay data from North Inlet, SC, Plum Island, MA (Morris et al. 2013), and Apalachicola, FL (Alizad et al. 2016) gave a feasible range of *S. alterniflora* growth as spanning from about 30 cm above mean high water (MHW) to 10 cm below mean sea-level (MSL).

Relative marsh elevation is an important determinant of productivity (Morris et al. 2002), and the vertical position of a saltmarsh within its growth range also determines its vulnerability to SLR. A related metric known as elevation capital was defined by Cahoon and Guntenspergen (2010) as the position of the wetland relative to the lowest elevation at which plants can survive (i.e., the bottom of the growth range). For example, a marsh will have 1 m of elevation capital when situated 1 m above its lower vertical limit. In the absence of any vertical accretion, sea level would need to rise 1 m before the marsh drowns, though it probably would not be healthy as it approached its lower limit. Thus, vertical growth range is proportional to tide range, and for comparative purposes, it is useful to normalize the growth range. Normalization of the elevations (*Z*) of SET stations and cells within digital elevation models (DEM) in each park was accomplished by dividing elevation (NAVD 88) by the growth range, and we refer to this as the normalized elevation capital (NEC), defined as:

$$NEC = (Z - (MSL - 10\ cm)) / ((MHW + 30\ cm) - (MSL - 10\ cm))$$

The NEC allows for a comparison of relative elevation and marsh status across sites independently of local tide range.

Lidar Elevations and Marsh NEC Frequency Distributions

Topobathy DEMs were generated by two different agencies for the study sites. The University of Rhode Island (URI) Environmental Data Center (EDC) used lidar data collected by National Oceanic and Atmospheric Administration (NOAA) National Geodetic Survey (NGS) to generate the topobathy DEMs for ASIS, FIIS, and GATE. The ASIS lidar data were collected in May 2014, while the FIIS and GATE lidar data were collected in January 2014. The US Geological Survey (USGS) Coastal and Marine Geology Program (CMGP) used a combination of topographic lidar data collected in August 2013 and the best available bathymetry from various sources to generate the CACO DEM. The ASIS, FIIS, and GATE data were projected in NAD1983 UTM Zone 18N with the NAVD88 geoid 12a; CACO data were all projected in NAD1983 UTM Zone 19N with the NAVD88 geoid 12a.

Marsh habitat was defined as any cell of the DEMs having a normalized elevation capital in the range of $0 < NEC \leq 1$. Cells had a resolution of 1 m. Subsequently, the frequency distribution of marsh NEC was computed from 21 equally distributed bins within $0 < NEC \leq 1$ for each park.

Vertical Accretion Rate

Vertical accretion rates were computed from empirical time series of SET measurements and were also calculated from the MEM. The empirical rates were calculated from linear regressions (SAS PROC REG v9.4) of elevation time series from

each SET station starting in 1998 to 2002 and continuing through 2015. Each regression returned a slope (the vertical accretion rate) and goodness-of-fit statistics. Several sites were restored by thin-layer sediment placement (TLP), and the pre-TLP and, to allow for compaction; 2-year post-treatment data were excluded from the analysis of long-term trends. The robustness of the regressions varied among sites, and those having a P value > 0.1 were excluded from the summary analyses shown here. Statistics on the complete set of regressions are shown in Table S2.

MEM was used to calculate vertical accretion rates for each SET site for each time point of the series and each elevation. The calculations were made using combinations of site-specific elevations and tidal datums, and generic model parameters: $m = 15$ mg/l, $q = 2.8$, and $k_r = 0.1$. We also used a generic biomass growth profile with a range between MSL − 10 cm and MHW + 30 cm, B_{max} of 1653 g/m^2, a root-shoot ratio of 2, and a below-ground turnover rate of 0.5/year. Thus, for each site, we computed a time series of dz/dt which was averaged by site. The site-specific means were then averaged by park.

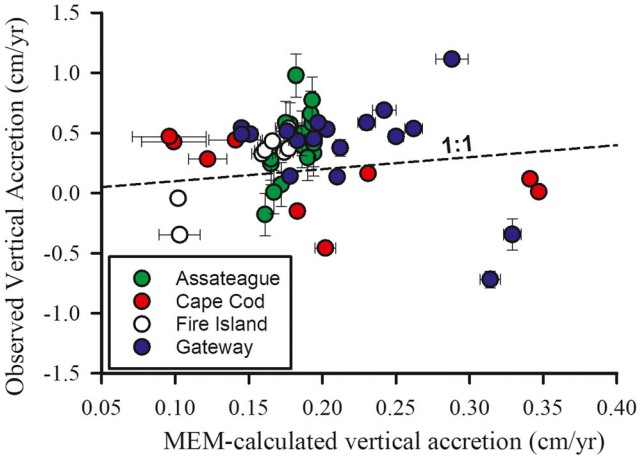

Fig. 4 The observed vertical accretion rates computed from individual SET sites is plotted against the MEM-calculated vertical accretion rates made with generic parameters as discussed in the text under Vertical Accretion Rates. Hence, model inputs differed only in the elevations and tidal datums used, which in turn resulted in different biomass values and sedimentation rates. Observed observations are the slopes of regressions (± 1 SE of regression slope). Calculated values are the means (± 1 SD) of rates computed for each elevation across the time series

Results

Observed and MEM-Calculated Vertical Accretion Rate

The grand mean of observed vertical accretion rates was 0.36 cm/year. This compared with a mean of MEM-calculated rates with generic parameters of 0.19 cm/year (Table 1). The computed rates were less variable than observed rates due to the relative uniformity of input data. The root-mean-square error (RMSE) of the residuals (prediction error) of computed rates vs a line of slope = 1 (Fig. 4) was 0.39 cm. Observed vertical accretion averaged by park ranged from 0.16 at CACO to 0.51 cm/year at ASIS while calculated rates averaged between 0.15 at FIIS to 0.22 cm/year at GATE (Table 1). The range of observed rates across all individual SET stations was − 0.7 to 1.1 cm/year, while the range of calculated rates was 0.1 to 0.34 cm/year (Fig. 4). The means of observed accretion rates in all parks were significantly different from zero, except CACO ($P > |t| = 0.2$). Among parks, only in ASIS was the observed accretion rate significantly different from the MEM-calculated rate ($P > |t| = 0.0001$). The mean net accretion rate (NAR, observed vertical accretion net of the regional rate of sea-level rise of 0.39 cm/year) overall sites and parks was − 0.03 ± 0.33 cm/year and not significantly different ($P > |t| = 0.54$) from the regional rate of sea-level rise (0.39 cm/year). Among parks, the only site with NAR > 0 (0.12 ± 0.21 cm/year) and marginally significant ($P > |t| = 0.07$) or having an accretion rate different from the

Table 1 Comparison of generic MEM-calculated accretion rates (cm/year) with observed rates (from the slope of linear regressions of SET elevation vs time). Also shown are the mean normalized elevation capitals of SET stations and of marsh landscape DEMs by park and the mean high water across SET sites (MHW). Results specific to each SET station are given in Table S2

Park	N	Mean (± 1 SD) MEM-calculated (cm/year)	N	Mean (± 1 SD) Obs. Vertical accretion rate (cm/year)†	Normalized Elev. Cap. SET sites (X ± 1 SD)	Normalized Elev. Cap. DEM (X ± 1 SD)	MHW (cm NAVD 88)
ASIS	16	0.18 ± 0.01	13	0.51 ± 0.21	0.40 ± 0.07	0.54 ± 0.26	11.2
CACO	9	0.20 ± 0.1	8	0.16 ± .33	0.54 ± 0.10	0.56 ± 0.23	113 ± 35
FIIS	9	0.15 ± 0.03	9	0.26 ± 0.28	0.35 ± 0.09	0.58 ± 0.22	30.7
GATE*	18	0.22 ± 0.05	18	0.39 ± 0.40	0.53 ± 0.17	0.53 ± 0.28	86.6
Grand Means	52	0.19 ± 0.06	48	0.36 ± 0.34	0.46 ± 0.15		

*Pre-TLP observations of treated-sites excluded

† Non-significant regression slopes ($P > 0.1$) were excluded

rate of sea-level rise was ASIS. The park with SET stations having the greatest loss of relative elevation was CACO with NAR = − 0.23 ± 0.32 cm/year.

The four parks in this study fall into four groups according to their local MHW (Table 1). Within each of these groups, SET station elevations exist within a vertical range lower than MHW (Fig. 5A). The scope for marsh elevation naturally increases as MHW increases, and among parks, there was a tendency for the elevation of SET stations to increase with MHW. All are lower than MHW + 30 cm, the assumed maximum of the vertical growth range, and all but GATE are lower than MHW. The optimum elevation (approximate elevation of B_{max}) bisected most observed SET elevation data (Fig. 5A). Likewise, there was a positive correlation between SET elevation, or marsh surface elevation, and NEC (Fig. 5B).

The vertical space available for growth is bisected by line representing the approximate elevation for maximum growth (B_{max} in Fig. 5A). As shown in Fig. 1, the region above B_{max} is stable, i.e., a rise in sea level will increase biomass and elevation. There are three stations belonging to GATE identified as "post TLP" where the elevations were raised to within the stable range by thin-layer sediment application (Fig. 5A). The TLP stations had accretion rates ranging from 0.14 to 0.59 cm/year. The SET elevations in all sites and all parks populate a range of NEC values that include both stable and unstable regions. Two parks, CACO and GATE, have sites with the highest NEC values in the stable range, but both also have sites in the unstable range.

Observed vertical accretion rates had no relationship to MHW (Fig. 5C). Within each of the four MHW groups, the range of observed accretion rates ranged from about − 0.5 to 1 cm/year. Vertical accretion rate also was not linearly related to NEC (Fig. 5D). In theory, vertical accretion should be a non-linear function of NEC as shown in Fig. 1B and, supporting this, a polynomial fit through the data in Fig. 5D

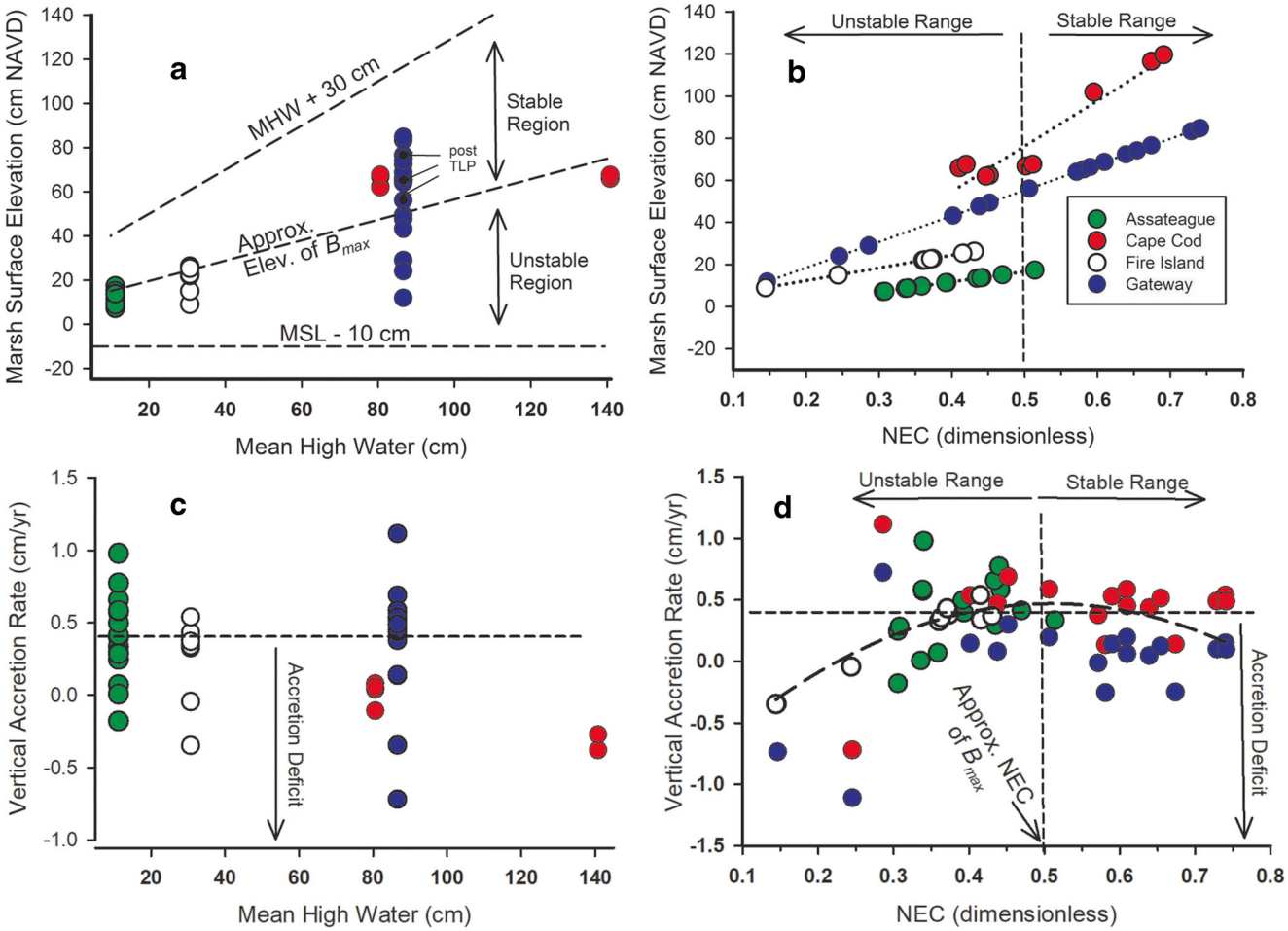

Fig. 5 Analyses of empirically derived vertical accretion rates (from SET platforms) in the four parks shown in the 5B legend. (A) The initial surface elevation of each SET site plotted against the local MHW. Also shown are the stable elevation range (above B_{max}), and suboptimal (unstable) growth range in relation to tidal datums. (B) The initial elevation each marsh surface at SET sites plotted against their normalized elevation capital (NEC). (C) Vertical accretion rate at each SET site plotted against the local MHW. The regional rate of sea-level rise is indicated by the dashed line. (D) The vertical accretion rate plotted against normalized elevation capital (NEC). Included is a best fit of a polynomial curve

was significant ($P < 0.02$, $R^2 = 0.17$). Overall, the SET stations were evenly split between the stable and unstable sides of NEC, with microtidal FIIS having all of its sites lower than NEC = 0.5 and GATE having the greatest proportion, 61%, of sites with NEC > 0.5 (Fig. 5B, D).

Normalized Elevation Capital and Net Accretion Rate

Marsh habitat in each park was classified on the basis of the growth range of *S. alterniflora* from a DEM, i.e., marsh was classified in each park on the basis of relative elevation. By definition, the growth range spans the full range of NECs between 0 and 1, and the definition and calculation of NEC did capture the majority of biomass samples from collections made in the parks (Fig. 6). All but 2.3% of samples were in NEC range 0 to 1. The frequency distribution of NECs on a landscape scale differed among parks. For example, FIIS has a higher proportion of NEC above 0.5, 64% (Fig. 7), in contrast with the relatively low positions of its SET stations (Fig. 5B, D). At the landscape scale, GATE has the lowest frequency above NEC = 0.5 at 53% (Fig. 7).

The current status of a marsh relative to SLR is captured by the accretion deficit or vertical accretion rate net of the rate of SLR (Fig. 5D). In theory, the NEC should be predictive of marsh response to an increase in rate (acceleration) of SLR—gain in productivity and elevation at NEC > 0.5, and with some loss in relative elevation, and loss in productivity and biogenic accretion at NEC < 0.5. Subtracting the regional rate of SLR from the observed accretion rates gives the net accretion rate (NAR), which was negative for two parks, with CACO having the lowest and ASIS having the sole positive average NAR. However, only ASIS and CACO had mean NAR marginally different from zero ($P > |t| = 0.07$ and 0.09, respectively), indicating that the average SET station is keeping pace with SLR in at least three of the four parks (Table 1).

Pre- and Post-sandy Results

There was little or no change in mean vertical accretion rate by park whether computed over the entire time series (to Oct 2015) of each SET station or from the start of the data record to the last pre-Sandy date (29 Oct 2012) (Table 2). Likewise, there were no significant differences in pre- and post-Sandy mean rates.

Three of the parks showed an average episodic gain in elevation exceeding their long-term averages and resulting from the storm (Table 3). The four parks recorded average episodic losses and gains from − 0.03 to 0.82 cm, corresponding to annualized rates of − 0.05 to 2.2 cm/year. SET stations in park GATE were least affected on average by the storm, while ASIS was most positively affected (Table 3). The standard deviations of average elevation gain were high in every park indicating that there was considerable within-park spatial variation in episodic accretion resulting from the storm (Table 3).

An analysis of vertical accretion rates by NEC bin class revealed that the greatest average vertical accretion rate, 0.43 cm/year, occurs in the range 0.4 < NEC < 0.6 (Table 4). The pre- and post-Sandy mean accretion rates were all positive, but not significantly different among NEC bin classes. The number of passing regressions (with $P < 0.1$) declined sharply from the complete, continuous time series to the pre- and post-Sandy series, which no doubt affected the results. At least the result from the continuous series with the greatest number of samples is consistent with a predicted trend (e.g., Figs. 1B and 5B).

The average, episodic gain in elevation immediately before and after the storm was positive in the optimum (0.4 to 0.6) NEC bin and trended downward at super-optimal and suboptimal levels of NEC (Table 5). The optimum NEC bin gained 0.61 ± 0.93 cm corresponding to an annualized rate of 3.7 cm/year, while the sub- and super-optimal NEC bin classes gained

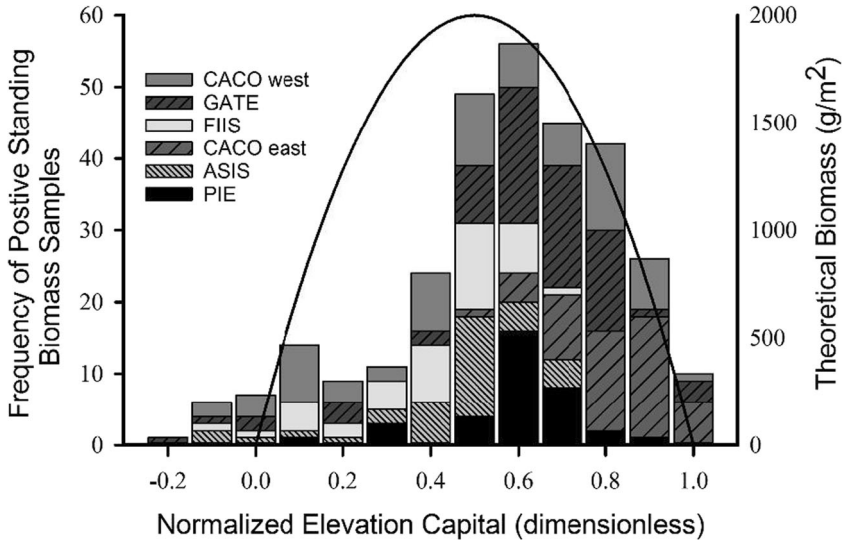

Fig. 6 Absolute counts of positive biomass samples from each park, including Plum Island Estuary, by NEC bin class (increments of 0.05) and the theoretical standing biomass curve extending from NEC = 0 to NEC = 1

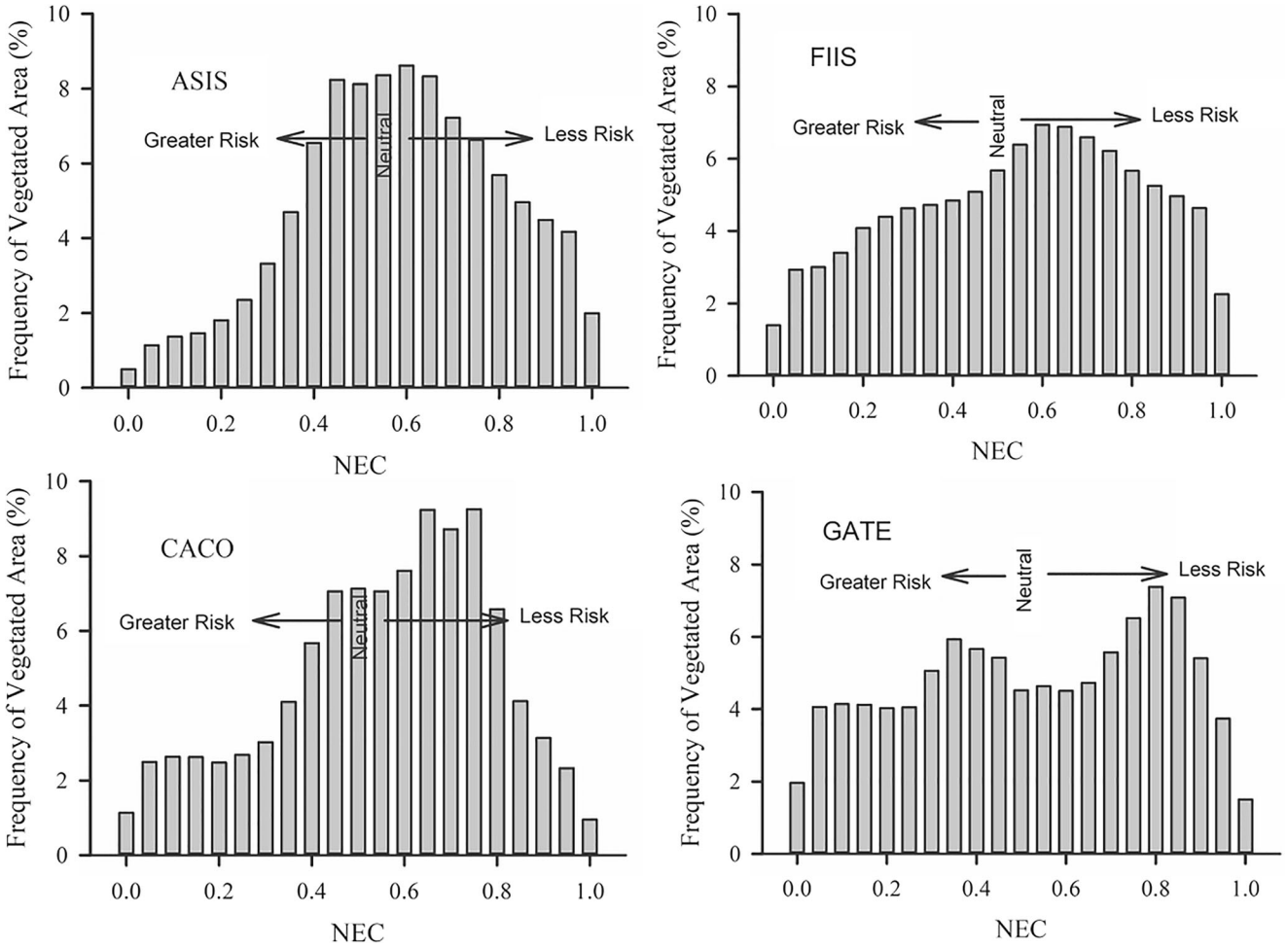

Fig. 7 Frequency distributions of normalized elevation capital across the marsh landscapes at ASIS, GATE, FIIS, and CACO in 2014. Areas where NEC > 0.5 are theoretically more stable: when SLR accelerates, they should gain elevation at a greater rate, but at a lower elevation. Areas where NEC < 0.5 are less stable: when SLR accelerates, biomass and biovolume production should decline, inorganic sedimentation should increase, and relative vertical elevation should decline

annualized rates of 0.87 and 0.05 cm/year, respectively (Table 5).

Response of Gateway TLP Sites to Sandy

Three SET stations in Gateway's Big Egg marsh ($N = 3$), restored by additions of sediment (TLP) in late 2003 (Cahoon et al. 2019), had mean pre- and post-Sandy vertical accretion rates of 0.16 and 0.36 cm/year, respectively (Table 6). The untreated marshes in Gateway had pre-and post-Sandy accretion rates of 0.48 and 0.57 cm/year. Pre- and post-Sandy accretion rates did not differ significantly among or within treatments. GATE TLP sites over the entire time series gained 0.29 cm/year compared with the mean of untreated GATE

Table 2 Mean vertical accretion rates by park from linear regressions of marsh elevation vs time from SET stations. The time series were parsed into pre- and post-Sandy periods. The number of stations (N) per park varies among sequences due to changes in the significance level of regressions

Park	Continuous from start to Oct 2015		Pre-Sandy < 29 Oct 2012		Post-Sandy > 29 Oct 2012	
	N	Mean (± 1 SD) slope (cm/year)	N	Mean (± 1 SD) slope (cm/year)	N	Mean (± 1 SD) slope (cm/year)
ASIS	13	0.51 ± 0.21	9	0.63 ± 0.28	6	0.34 ± 0.12
CACO	8	0.16 ± 0.33	9	0.14 ± 0.31	5	0.15 ± 0.56
FIIS	9	0.26 ± 0.28	9	0.20 ± 0.26	4	0.16 ± 0.55
GATE	18	0.39 ± 0.40	17	0.42 ± 0.36	15	0.53 ± 0.50

Table 3 Mean episodic change and annualized change in marsh elevation by park between the last pre-Sandy measurement and the first post-Sandy measurement

Park	*N*	Δ Elevation (cm)	Annualized rate (cm/year)
ASIS	16	0.82 ± 0.90	2.16 ± 3.1
CACO	9	0.24 ± 0.67	0.41 ± 1.14
FIIS	9	0.63 ± 1.06	8.5 ± 14.4
GATE	18	− 0.03 ± 0.44	− 0.05 ± 3.5

Table 5 Mean episodic change in marsh elevation by NEC bin class between the last pre-Sandy measurement and the first post-Sandy measurement. Means were computed over all sites in all parks

NEC bin	*N*	Δ Elevation (cm)	Annualized rate (cm/year)
<= 0.4	12	0.28 ± 0.85	0.87 ± 4.36
> .4 and < .6	28	0.61 ± 0.93	3.7 ± 8.8
>= .6	12	0.01 ± 0.19	0.05 ± 1.51

sites ($N = 15$) of 0.41, but the difference in the annual accretion rates by treatment was not significant ($P > |t| = 0.5$). We do not know what the accretion rates of the TLP sites were before treatment, though we assume that they must have been considerably less because they had lost relative elevation to the point of needing restoration.

Generalizations from Marsh Equilibrium Theory

The model was solved for $\frac{dz}{dt}$, $\frac{dz_{org}}{dt}$, and $\frac{dz_{min}}{dt}$ using a generic set of parameter values q, k, B_{TR}, R_{RS}, and biomass distribution as discussed earlier, and permutations of NEC and MHW. This resulted in predicted accretion rates shown in Fig. 8. Total accretion increases with MHW, especially at low NEC (Fig. 8A). It is highest at the highest MHW (120 cm in this example), and NEC = 0.3 (Fig. 8C). At low MHW, accretion is greatest at NEC = 0.5. These responses are explained by parsing them into their organic and inorganic components (Fig. 8B). Considering only the mineral component, the greatest mineral accretion occurs at the highest MHW and lowest NEC. As NEC approaches 1, mineral accretion approaches 0, irrespective of MHW. By contrast, organic accretion is solely dependent on NEC, and follows the biomass distribution that spans the vertical range $0 < \text{NEC} < 1$, consistent with biomass collections in the parks (Fig. 6). The assumption is made, with support from empirical studies (Morris et al. 2013), that maximum biomass occurs in the middle of this range. The vertical gain in elevation is derived by dividing the mass input of inorganic matter $0.5 \times q \times m \times f \times D \times F_{IT}$ by its self-packing density k_2 and the organic input $k_r \times R_{RS} \times B_{TR} \times B_S$ by its self-packing density k_1. The self-packing densities of organic and inorganic matter, 0.085 and 1.99 g/cm^3 (Morris et al. 2016), respectively, imply that 1 g dry organic matter occupies 23× more volume on average than 1 g of dry mineral sediment. Consequently, the low mineral concentrations that characterize these parks contribute little volume growth to marsh sediment, except at low NEC and high MHW, and the major contribution to volume growth is from the accretion of refractory organic production of roots and rhizomes which is maximal near NEC = 0.5.

Discussion

There is great variability within the marshes of each park in the spatial distribution of NEC (Fig. 7) as determined from digital elevation models (DEMs) and local tidal datums. The variability is expected because across any marsh landscape the elevation must span the full vertical growth range of the vegetation. This implies that any marsh landscape will have areas with varying levels of risk from SLR. The lower the NEC, the more vulnerable a marsh at that location is to SLR. Marsh equilibrium theory predicts that a marsh with NEC > 0.5 will have a vertical accretion that increases as the rate of SLR increases, or negative feedback, while a marsh with NEC < 0.5 should have biogenic accretion that decreases with rising rate of SLR, or positive feedback. If relative marsh elevation is super-optimal for growth, at high NEC, an increase in relative sea level will stimulate growth and, consequently, the biogenic accretion of soil as well as mineral sedimentation will increase (Fig. 2). On the suboptimal side of the growth curve, an increase in flooding will decrease productivity and biovolume

Table 4 Mean vertical accretion rates by NEC bin class from linear regressions of marsh elevation vs time from SET stations. The time series were parsed into pre- and post-Sandy periods. Means were computed over all sites in all parks, except those in tidally restricted areas

Continuous from start to Oct 2015			Pre-Sandy < 29 Oct 2012		Post-Sandy	
NEC bin	*N*	Mean (± 1 SD) slope (cm/year)	*N*	Mean (± 1 SD) slope (cm/year)	*N*	Mean (± 1 SD) slope (cm/year)
<= 0.4	16	0.29 ± 0.47	12	0.37 ± 0.51	5	0.54 ± 1.03
> 4 and < .6	22	0.43 ± 0.17	22	0.39 ± 0.25	14	0.38 ± 0.32
>= .6	10	0.30 ± 0.34	10	0.31 ± 0.37	11	0.30 ± 0.29

Table 6 Mean vertical accretion rates (cm/year) by treatment (restored by thin-layer placement (TLP) or not) in Gateway park during the pre- (< 29 Oct 2012) and post-Hurricane Sandy periods, and the episodic change between the last pre-Sandy measurement and the first post-Sandy measurement

Treatment	Starting time to Oct 2015	Start to Oct 2015		Pre-Sandy		Post-Sandy		Episodic change	
		N	Slope *X* ± 1 SD	*N*	Slope *X* ± 1 SD	*N*	Slope *X* ± 1 SD	*N*	Δ Elevation *X* ± 1 SD (cm)
Untreated	2002–2006	15	0.41 ± 0.43	14	0.48 ± 0.37	12	0.57 ± 0.54	15	− 0.04 ± 0.48
TLP-restored	2009	3	0.29 ± 0.26	3	0.16 ± 0.13	3	0.36 ± 0.31	3	0.06 ± 0.05

accretion. The decrease is a result of the negative response of the vegetation to an increase in hydroperiod or flood duration that occurs at low NEC. Mineral sedimentation may increase, but at the low concentrations of suspended sediment that characterize these northeast marshes (Weston 2014; Peteet et al. 2018), biovolume growth is more important than mineral sedimentation (Morris et al. 2016 and Fig. 8). However, note that the vertical accretion rate of a site where NEC < 0.5 can be greater than a site where NEC > 0.5. For example, vertical accretion on a site with NEC = 0.9 will be less than on a site with NEC = 0.4, as seen in Fig. 1B where the accretion rate of point b is greater than the accretion rate of point a. But the elevation (Fig. 1C) and productivity (Fig. 1A) at point b will be declining rapidly as the rate of SLR increases. The vertical position of the marsh surface, whether at point a or b, will depend on the rate of SLR.

As noted above, at a given MHW level, a marsh high within its growth range (high NEC) is more stable than a marsh lower in its range. Thus, when NEC = 0, marsh elevation *Z* is at the lower limit for *S. alterniflora* growth, and when NEC = 1, marsh elevation is at the upper limit for growth. At a landscape scale, parks with the highest frequencies of NEC above 0.5 were FIIS and CACO with 64% and 63% of total marsh area in the stable region. GATE and ASIS had 53% and 59% of area above NEC 0.5. With further acceleration of SLR, these frequency distributions will change, and MEM informs us how this happen. Those areas with NEC < 0.5 will lose relative elevation more rapidly than areas with NEC > 0.5. With continued acceleration in SLR, eventually the stable marshes (NEC > 0.5) will cross over to the suboptimal side of the curve. The net effect will be a transformation of the NEC distributions shown in Fig. 7 towards right-skewness as the greater proportion of area slips to the suboptimal side of the distribution.

Subtracting a regional rate of SLR of 0.39 cm/year from the vertical accretion rates of SET stations gave an average NAR of about zero. Even in ASIS, its 0.5 cm/year average accretion rate (Table 1) was only marginally different from the rate of SLR ($P > |t| = 0.07$) despite being microtidal. But its NEC is within that optimal range from 0.4 to 0.6 where observed and predicted accretion rates should be maximal. This suggests that these wetlands will not tolerate higher rates of SLR. If sea level rises more quickly than the marshes can equilibrate or to a level that moves them to the suboptimal side of the growth curve, then by definition their accretion rates will be less than SLR. Thus, the transition to right-skewness is in progress. Monitoring of their NEC frequency distributions on a landscape scale with lidar or similar technologies should be a useful method of assessing the stability of a marsh.

The combination of low tide range and low elevation capitals put marshes at risk for collapse in the face of accelerating SLR (Reed 1995; Cahoon and Guntenspergen 2010; Kirwan and Guntenspergen 2010; Morris et al. 2012; Cahoon et al. 2019). Assateague and Fire Island are most vulnerable to higher SLR scenarios by virtue of their low MHW levels (ca. 11 cm at ASIS and 31 cm at FIIS). In contrast, Cape Cod and Gateway have wider tide ranges (Table 1). These two parks have a more favorable combination of factors important for survival. However, as noted above, having high MHW and high NEC do not guarantee that a marsh will be in equilibrium with SLR (NAR = 0) or will have positive NAR.

An important caveat relative to these analyses is that the regional rate of SLR from the NOAA gages may differ from the contemporary local rates. In addition, NEC calculations for low tidal range marshes are very sensitive to tidal datums. A small tide range will amplify errors in NEC resulting from small errors in tidal datums. Consequently, for modeling or interpreting NEC data, it is important to have good, local measurements of the tides from which NEC is derived. For SET sites, this can be accomplished with water level recorders; for the landscape scale, it is practical to make tidal calculations from hydrodynamic models or from satellite observations of water level.

There does not appear to be a single metric that can describe the vertical accretion rates observed at the SET stations in these parks. The reason is that accretion rate (*dz/dt*) is a multidimensional function. It depends on local productivity, relative elevation, suspended sediments, local hydrology, and so on. Its complexity is revealed by a plot of *dz/dt* vs NEC and MHW (Fig. 8), computed using generic constants in the model. In this case, we solved the model with permutations of NEC varying from 0 to 1 and MHW varying from 5 to 120 cm, and calculated *dz/dt* for each combination. We found that accretion was greatest at the highest MHW (120 cm), conditioned on NEC. Even at near zero NEC, the vertical accretion rate at 120 cm MHW was about 0.35 cm/year (Fig.

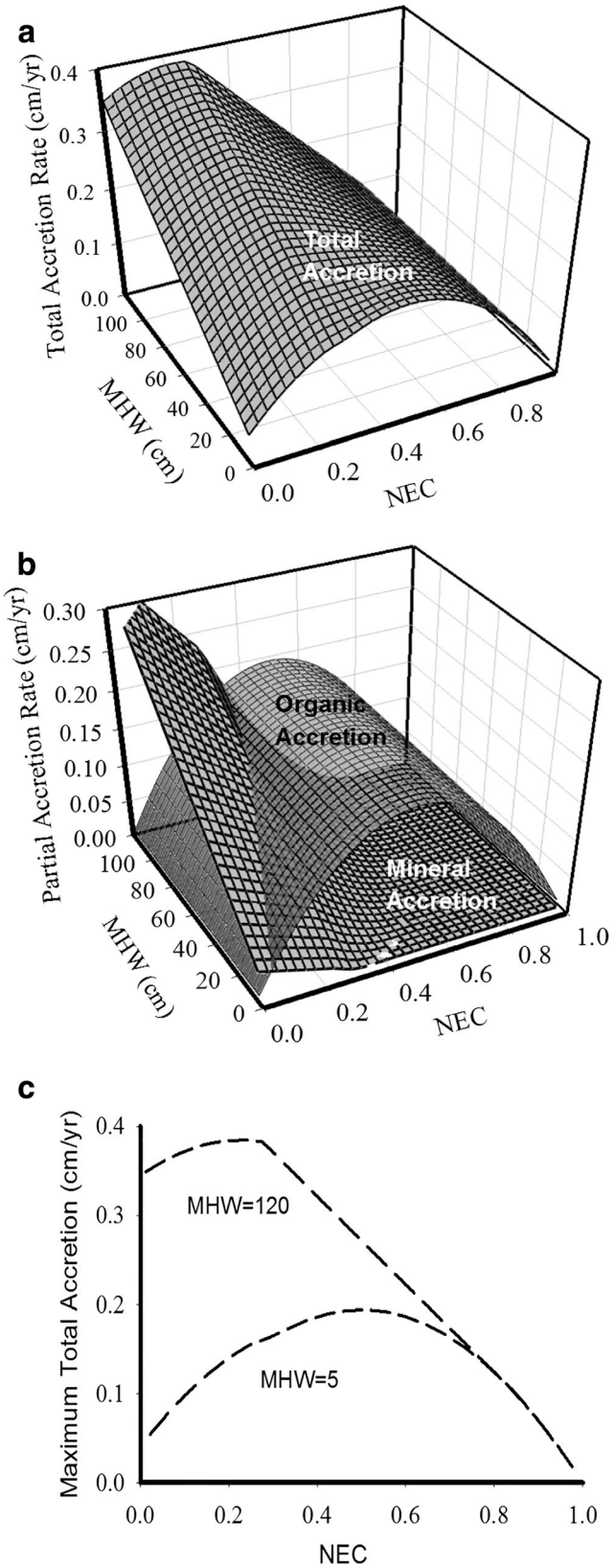

Fig. 8 MEM solutions resulting from permutations of NEC and MHW using generic parameters as in Fig. 4. Total vertical accretion rate (dz/dt) is shown in (A), the partials (dz_{min}/dt and dz_{org}/dt) in panel (B), and shown in (C) are the maximum dz/dt from (A) at MHW = 5 and 120 cm

8C). In this case, mineral sediment is all important, because settling of suspended sediment from a 120 cm water column can be substantial. The highest accretion rate among all permutations, 0.39 cm/year, was also at the highest MHW, but at NEC = 0.225 where biovolume production is still significant (Fig. 8B). At NEC = 0.5, the model returned a total accretion rate of 0.2 cm/year. At low MHW, this was exclusively the result of biovolume production. These accretion rates equal or exceed the rate of SLR from past centuries, and therefore we would expect these marshes to have sediment composed of peat and to be situated today at a relatively high elevation, but falling. At MHW = 120 cm, biovolume production (peat) accounts for all of the accretion at NEC > 0.81, but at rates < 0.12 cm/year. At low MHW, the simulations produce peat marshes when NEC > 0.33 and dz/dt<0.2 cm/year. Thus, peat marshes are possible at the highest elevations across a spectrum of tides, provided rates of SLR are low enough. Furthermore, microtidal marshes will produce peat at higher rates of SLR than macrotidal marshes due to differences in the volume of water flooding the marshes and, thus, to differences in sediment loading.

Generalities emerge from Marsh Equilibrium Theory (Fig. 8) help to explain some of the trends in vertical accretion. For example, the long-term accretion rates were greatest for sites in the range 0.4 < NEC < 0.6 (Table 4). This also was true of the episodic rate of elevation gain during the storm (Table 5), though it is not entirely clear why this was the case unless high biomass in the 0.4 < NEC < 0.6 range filtered more sediment. In theory, the long-term accretion rate in these marshes should be dominated by organic accretion (Fig. 8B), but the episodic gain during the storm was from mineral deposition, which normally would be greatest at low NEC (Fig. 8A). If plant biomass was greatest at NEC = 0.5, the standing biomass could have captured more sediment. Observed vertical accretion rates had no relation to MHW (Fig. 5C), which may be surprising given that MHW should be a proxy for tidal energy, and therefore sediment loading. However, the long-term accretion in these marshes appears to be dominated by organic accretion, and the storm apparently had little impact on this (Table 2). In fact, the storm appears to have been a non-event relative to the responses of SET stations. Note, however, we are generalizing about the SET stations in these marshes, which may or may not be representative of entire marsh landscapes.

The practice of thin-layer placement (TLP) is a method of supplying sediment to subsiding marshes by spraying a sediment slurry under high pressure over the marsh surface (Ray 2007) as was done at the GATE Big Egg marsh restoration site. This practice does not add new sediment to the estuary, because the sediment is taken from a nearby channel or creek, and consequently it has been argued that removal of sediment from one part of a system (a tidal channel) to nourish another (a marsh) may be counterproductive (Ganju 2019).

Ultimately, marshes are not sustainable in the face of accelerating SLR in the absence of new sediment. In fact, spatially explicit simulations of these parks with MEM, adding an acceleration of SLR to a level of 1 m this century, predict modest gains in marsh areas early in the century as marshes migrate to higher elevations, followed by major losses as marshes drown (Morris and Renken 2019). However, sediment additions can maintain marshes at an elevation favorable to marsh vegetation, albeit with an ever-expanding subtidal area. Our analysis suggests that restoring the elevation capital of a marsh by TLP can restore biogenic accretion and raise the rate of vertical accretion (Fig. 8). Furthermore, TLP can maintain marshes at an elevation favorable to the marsh community writ large and beneficial to at-risk species such as the saltmarsh sparrow. Thus, TLP is a good management tool for sustaining immediately threatened marsh habitat and is preferable to the practice of dredge spoil *disposal* techniques that effectively remove sediment from the system. Good candidate sites for TLP are those with low NEC.

Theory predicts that adjustment of marsh elevation from low NEC to middle or higher NEC by sediment addition should restore the capacity of a marsh to increase vertical accretion by growth of biovolume. This is consistent with the responses of SET stations in the restored marsh at GATE. The pre-restoration accretion rate in this marsh ranged from − 0.35 to 0 cm/year (not shown), but none had slopes differing significantly from zero and there were only four measurements made during a single year preceding the treatment. However, because about 45 cm of sediment was needed to bring this marsh to an elevation favorable for *Spartina alterniflora* (Cahoon et al. 2019), we can assume that this marsh had been losing elevation for some time, and raising the elevation resulted in a positive average accretion rate (Table 6). Post-Sandy accretion rates (2012–2015) were also similar, 0.36 ± 0.54 and 0.57 ± 0.54 cm/year in restored and not-restored marshes, respectively. Post-restoration, pre-Sandy rates in restored marshes and not-restored GATE marshes were 0.16 ± 0.13 and 0.48 ± 0.37 cm/year, respectively, and not significantly different. Thus, the trends support the theory, but other factors besides relative elevation may also be important here such as impacts from urbanization (Hartig et al. 2002; Wigand et al. 2014). Future studies should monitor the standing biomass, marsh elevation, and soil organic matter at these sites.

With advances in lidar, drone, and satellite technology, it should be possible to monitor elevations across entire landscapes and changes in plant communities. The frequency distribution and especially the change in distribution of relative elevations will be a powerful diagnostic tool. In a mature marsh, distributions of relative elevation with positive skew (left-leaning curve with long right tail) will be characteristic of a deteriorating marsh. A frequency distribution of relative elevations with negative skew (left tail) will be characteristic of a marsh that has been successfully tracking sea level. A normal distribution, as was the case at North Inlet (Morris et al. 2005), is probably a signal that the marsh is in transition. Any temporal change in the direction of the curve will also be a good diagnostic. Application of this technique to different marsh units within an estuarine landscape also would be useful in identifying those areas at risk, and therefore good candidates for TLP. Improvements in satellite technology now allow the classification of marsh landscapes and detection of marsh community change, erosion/accretion of creekbanks or, in conjunction with lidar data, vertical biomass profiles (Miller et al. 2019).

Acknowledgments The authors acknowledge the assistance of Andrew Neil and Scott Rasmussen (University of Rhode Island, Environmental Data Center), and James Edwards and Gail Pruss (University of South Carolina). We thank Dennis Whigham and two anonymous reviewers for helpful criticisms and suggestions.

Funding Information This work was financially supported by the National Park Service Northeastern Coastal and Barrier Network Grant Number: P15AC00006, National Science Foundation LTREB grant 1654853, and NA16NOS4780208 from the National Oceanic and Atmospheric Administration (NOAA). Endorsement by neither the NPS nor NOAA is not implied.

References

Alizad, K., S.C. Hagen, J.T. Morris, S.C. Medeiros, M.V. Bilskie, and J.F. Weishampel. 2016. Coastal wetland response to sea level rise in a fluvial estuarine system. *Earth's Future* 4 (11): 483–497. https://doi.org/10.1002/2016EF000385.

Alizad, K., S.C. Hagen, S.C. Medeiros, M.V. Bilskie, J.T. Morris, L. Balthis, and C.A. Buckel. 2018. Dynamic responses and implications to coastal wetlands and the surrounding regions under sea level rise. *PLoS One* 13 (10): e0205176.

Arkema, K.K., G. Guannel, G. Verutes, S.A. Wood, A. Guerry, M. Ruckelshaus, P. Kareiva, M. Lacayo, and J.M. Silver. 2013. Coastal habitats shield people and property from sea-level rise and storms. *Nature Climate Change* 3 (10): 913–918. https://doi.org/10.1038/nclimate1944.

Blake, E. S., Kimberlain, T. B., Berg, R. J., Cangialosi, J. P., and Beven, J. L., II. 2013. Tropical cyclone report: Hurricane Sandy (AL182012) 22–29 October 2012. National Oceanic and Atmospheric Administration, National Hurricane Center.

Bouchard, V., and J.C. Lefeuvre. 2000. Primary production and macro–detritus dynamics in a European salt marsh: Carbon and nitrogen budgets. *Aquatic Botany* 67 (1): 23–42.

Buth, G.J.C., and L.A.C.J. Voesenek. 1987. Decomposition of standing and fallen litter of halophytes in a Dutch salt marsh. In *Geobotany 11: Vegetation between land and sea*, ed. A.H.L. Huiskes, C.W.P.M. Blom, and J. Rozema, 146–165. Dordrecht: Dr. W. Junk Pub.

Cahoon, D., and G. Guntenspergen. 2010. Climate change, sea-level rise, and coastal wetlands. *National Wetlands Newsletter* 32: 8–12.

Cahoon, D.R., J.C. Lynch, C.T. Roman, J.P. Schmit, and D.E. Skidds. 2019. Evaluating the relationship among wetland vertical development, elevation capital, sea-level rise, and tidal marsh sustainability. *Estuaries and Coasts* 42 (1): 1–15. https://doi.org/10.1007/s12237-018-0448-x.

Chalmers, A.G., R.G. Wiegert, and P.L. Wolf. 1985. Carbon balance in a salt marsh: Interactions of diffusive export, tidal deposition and rainfall-caused erosion. *Estuarine, Coastal and Shelf Science* 21 (6): 757–771.

Costanza, R., M. Wilson, A. Troy, A. Volnov, S. Liu, and J. D'Agostino. 2006. *The value of New Jersey's ecosystem services and natural captial. Trenton, NJ: New Jersey Department of Environmental Protection*. Burlington, VT: Gund Institute for Ecological Economics.

Darby, F.A., and R.E. Turner. 2008. Below- and aboveground biomass of *Spartina alterniflora*: Response to nutrient addition. *Estuaries and Coasts* 31 (2): 326–334.

Ganju, N.K. 2019. Marshes are the new beaches: Integrating sediment transport into restoration planning. *Estuaries and Coasts* 42 (4): 917–926. https://doi.org/10.1007/s12237-019-00531-3.

Hartig, E.K., V. Gornitz, A. Kolker, F. Mushacke, and D. Fallon. 2002. Anthropogenic and climate-change impacts on salt marshes of Jamaica Bay, New York City. *Wetlands* 22 (1): 71–89.

Hodson, R.E., R.R. Christian, and A.E. Maccubbin. 1984. Lignocellulose and lignin in the salt marsh grass *Spartina alterniflor*a: Initial concentrations and short-term, post-depositional changes in detrital matter. *Marine Biology* 81 (1): 1–7.

Kirwan, M.L., and G.R. Guntenspergen. 2010. Influence of tidal range on the stability of coastal marshland. *Journal of Geophysical Research* 115 (F2): F02009. https://doi.org/10.1029/2009JF001400.

McKee, K.L., and W. Patrick Jr. 1988. The relationship of smooth cordgrass (*Spartina alterniflora*) to tidal datums: A review. *Estuaries* 11 (3): 143–151.

Mendelssohn, I.A., and J.T. Morris. 2000. Eco-physiological controls on the productivity of *Spartina alterniflora* Loisel. In *Concepts and controversies in tidal marsh ecology*, ed. M.P. Weinstein and D.A. Kreeger, 59–80. Boston, MA: Kluwer Academic Publishers.

Miller, G.J., J.T. Morris, and C. Wang. 2019. Estimating aboveground biomass and its spatial distribution in coastal wetlands utilizing planet multispectral imagery. *Remote Sensing* 11 (17): 2020. https://doi.org/10.3390/rs11172020.

Morris, J.T. 1982. A model of growth responses by *Spartina alterniflora* to nitrogen limitation. *Journal of Ecology* 70 (1): 25–42.

Morris, J. T., and K. A. Renken. 2019. The impact of sea-level rise on saltmarsh condition and resiliency: Assateague Island National Seashore, Cape Cod National Seashore, Fire Island National Seashore, and Gateway National Recreation Area. Natural Resource Report NPS/NCBN/NRR—2019/1974. National Park Service, Fort Collins, Colorado.

Morris, J.T., P.V. Sundareshwar, C.T. Nietch, B. Kjerfve, and D.R. Cahoon. 2002. Responses of coastal wetlands to rising sea level. *Ecology* 83 (10): 2869–2877.

Morris, J.T., D. Porter, M. Neet, P.A. Noble, L. Schmidt, L.A. Lapine, and J. Jensen. 2005. Integrating LIDAR elevation data, multispectral imagery and neural network modeling for marsh classification. Int. J. *Remote Sensing* 26 (23): 5221–5234.

Morris, J.T., Edwards, J., Crooks, S., Reyes, E. 2012. Assessment of carbon sequestration potential in coastal wetlands. Pp 517-531. In: Recarbonization of the biosphere: ecosystem and global carbon cycle. R. Lal, K. Lorenz, R. Hüttl, B. U. Schneider, J. von Braun (eds). Springer.

Morris, J.T., K. Sundberg, and C.S. Hopkinson. 2013. Salt marsh primary production and its responses to relative sea level and nutrients in estuaries at Plum Island, Massachusetts, and North Inlet, South Carolina, USA. *Oceanography* 26 (3): 78–84.

Morris, J.T., D.C. Barber, J.C. Callaway, R. Chambers, S.C. Hagen, C.S. Hopkinson, B.J. Johnson, P. Megonigal, S.C. Neubauer, T. Troxler, and C. Wigand. 2016. Contributions of organic and inorganic matter to sediment volume and accretion in tidal wetlands at steady state. *Earth's Future* 4 (4): 110–121. https://doi.org/10.1002/2015EF000334.

Narayan, S., M.W. Beck, P. Wilson, C.J. Thomas, A. Guerrero, C.C. Shepard, B.G. Reguero, G. Franco, J.C. Ingram, and D. Trespalacios. 2017. The value of coastal wetlands for flood damage reduction in the northeastern USA. *Scientific Reports* 7 (1): 9463.

National Research Council. 1987. *Responding to changes in sea level: Engineering implications*. Washington, DC: The National Academies Press. https://doi.org/10.17226/1006.

Peteet, D.M., J. Nichols, T. Kenns, C. Chang, J. Browne, M. Reza, S. Kovari, L. Liberman, and S. Stern-Protz. 2018. Sediment starvation destroys New York City marshes' resistance to sea level rise. *PNAS* 115 (41): 10281–10286.

Ray, G.L. 2007. *Thin layer disposal of dredged material on marshes: A review of the technical and scientific literature. ERDC/EL technical notes collection (ERDC/EL TN-07-1)*. Vicksburg: U.S. Army Engineer Research and Development Center.

Reed, D.J. 1995. The response of coastal marshes to sea-level rise: Survival or submergence. *Earth Surface Processes and Landforms* 20 (1): 39–48.

Teal, J.M. 1962. Energy flow in the salt marsh ecosystem of Georgia. *Ecology* 43 (4): 614–624.

Weston, N.B. 2014. Declining sediments and rising seas: An unfortunate convergence for tidal wetlands. *Estuaries and Coasts* 37 (1): 1–23.

Wigand, C., C.T. Roman, E. Davey, M. Stolt, R. Johnson, A. Hanson, E.B. Watson, S.B. Moran, D.R. Cahoon, J.C. Lynch, and P. Rafferty. 2014. Below the disappearing marshes of an urban estuary: Historic nitrogen trends and soil structure. *Ecological Applications* 24 (4): 633–649.

Wilson, J.O., R. Buchsbaum, I. Valiela, and T. Swain. 1986. Decomposition in salt marsh ecosystems: Phenolic dynamics during decay of litter of *Spartina a1terniflora*. *Marine Ecology Progress Series* 29: 177–187.